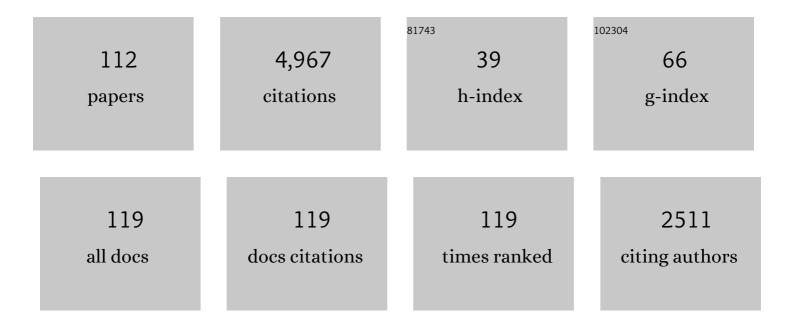
Xiu-Mian Hu

List of Publications by Year in descending order

Source: https://exaly.com/author-pdf/4981968/publications.pdf Version: 2024-02-01



Χιμ-Μιλη Ημ

#	Article	IF	CITATIONS
1	The timing of India-Asia collision onset – Facts, theories, controversies. Earth-Science Reviews, 2016, 160, 264-299.	4.0	572
2	Direct stratigraphic dating of India-Asia collision onset at the Selandian (middle Paleocene, 59 ± 1 Ma). Geology, 2015, 43, 859-862.	2.0	330
3	Review: Short-term sea-level changes in a greenhouse world — A view from the Cretaceous. Palaeogeography, Palaeoclimatology, Palaeoecology, 2016, 441, 393-411.	1.0	139
4	Sedimentary and tectonic evolution of the southern Qiangtang basin: Implications for the Lhasaâ€Qiangtang collision timing. Journal of Geophysical Research: Solid Earth, 2017, 122, 4790-4813.	1.4	137
5	Provenance of Lower Cretaceous Wölong Volcaniclastics in the Tibetan Tethyan Himalaya: Implications for the final breakup of Eastern Gondwana. Sedimentary Geology, 2010, 223, 193-205.	1.0	135
6	Upper Cretaceous oceanic red beds (CORBs) in the Tethys: occurrences, lithofacies, age, and environments. Cretaceous Research, 2005, 26, 3-20.	0.6	133
7	Xigaze forearc basin revisited (South Tibet): Provenance changes and origin of the Xigaze Ophiolite. Bulletin of the Geological Society of America, 2014, 126, 1595-1613.	1.6	132
8	Late Cretaceousâ€Palaeogene stratigraphic and basin evolution in the Zhepure Mountain of southern Tibet: implications for the timing of Indiaâ€Asia initial collision. Basin Research, 2012, 24, 520-543.	1.3	116
9	New insights into the timing of the India – Asia collision from the Paleogene Quxia and Jialazi formations of the Xigaze forearc basin, South Tibet. Gondwana Research, 2016, 32, 76-92.	3.0	115
10	Provenance of the Upper Cretaceous–Eocene Deep-Water Sandstones in Sangdanlin, Southern Tibet: Constraints on the Timing of Initial India-Asia Collision. Journal of Geology, 2011, 119, 293-309.	0.7	114
11	Upper Cretaceous oceanic red beds in southern Tibet: a major change from anoxic to oxic, deep-sea environments. Cretaceous Research, 2005, 26, 21-32.	0.6	106
12	Latest marine horizon north of Qomolangma (Mt Everest): implications for closure of Tethys seaway and collision tectonics. Terra Nova, 2002, 14, 114-120.	0.9	96
13	The birth of the Xigaze forearc basin in southern Tibet. Earth and Planetary Science Letters, 2017, 465, 38-47.	1.8	90
14	Cretaceous oceanic red beds as possible consequence of oceanic anoxic events. Sedimentary Geology, 2011, 235, 27-37.	1.0	83
15	Constraining the timing of the India-Asia continental collision by the sedimentary record. Science China Earth Sciences, 2017, 60, 603-625.	2.3	82
16	A transfer learning method for automatic identification of sandstone microscopic images. Computers and Geosciences, 2017, 103, 111-121.	2.0	80
17	Upper Cretaceous carbon- and oxygen-isotope stratigraphy of hemipelagic carbonate facies from southern Tibet, China. Journal of the Geological Society, 2006, 163, 375-382.	0.9	79
18	Upper Jurassic–Lower Cretaceous stratigraphy in south-eastern Tibet: a comparison with the western Himalayas. Cretaceous Research, 2008, 29, 301-315.	0.6	76

#	Article	IF	CITATIONS
19	Upper Triassic turbidites of the northern Tethyan Himalaya (Langjiexue Group): The terminal of a sediment-routing system sourced in the Gondwanide Orogen. Gondwana Research, 2016, 34, 84-98.	3.0	70
20	Cretaceous oceanic red beds (CORBs): Different time scales and models of origin. Earth-Science Reviews, 2012, 115, 217-248.	4.0	66
21	Marine rapid environmental/climatic change in the Cretaceous greenhouse world. Cretaceous Research, 2012, 38, 1-6.	0.6	65
22	Thickened juvenile lower crust-derived ~ 90 Ma adakitic rocks in the central Lhasa terrane, Tibet. Lithos, 2015, 224-225, 225-239.	0.6	65
23	Mid-Cretaceous oceanic red beds in the Umbria–Marche Basin, central Italy: Constraints on paleoceanography and paleoclimate. Palaeogeography, Palaeoclimatology, Palaeoecology, 2006, 233, 163-186.	1.0	62
24	Sandstone provenance and tectonic evolution of the Xiukang Mélange from Neotethyan subduction to India–Asia collision (Yarlung-Zangbo suture, south Tibet). Gondwana Research, 2017, 41, 222-234.	3.0	58
25	New Precise Dating of the Indiaâ€Asia Collision in the Tibetan Himalaya at 61ÂMa. Geophysical Research Letters, 2021, 48, e2020GL090641.	1.5	58
26	Early Cretaceous sedimentary evolution of the northern Lhasa terrane and the timing of initial Lhasa-Qiangtang collision. Gondwana Research, 2019, 73, 136-152.	3.0	57
27	Stratigraphic transition and palaeoenvironmental changes from the Aptian oceanic anoxic event 1a (OAE1a) to the oceanic red bed 1 (ORB1) in the Yenicesihlar section, central Turkey. Cretaceous Research, 2012, 38, 40-51.	0.6	56
28	Latest Cretaceous Himalayan tectonics: Obduction, collision or Deccan-related uplift?. Gondwana Research, 2015, 28, 165-178.	3.0	55
29	The Deep-Time Digital Earth program: data-driven discovery in geosciences. National Science Review, 2021, 8, nwab027.	4.6	55
30	The Cenomanian–Turonian anoxic event in southern Tibet. Cretaceous Research, 2001, 22, 481-490.	0.6	53
31	Exploring a lost ocean in the Tibetan Plateau: Birth, growth, and demise of the Bangong-Nujiang Ocean. Earth-Science Reviews, 2022, 229, 104031.	4.0	53
32	Upper Oligocene–Lower Miocene Gangrinboche Conglomerate in the Xigaze Area, Southern Tibet: Implications for Himalayan Uplift and Paleo-Yarlung-Zangbo Initiation. Journal of Geology, 2013, 121, 425-444.	0.7	52
33	Paleolatitudes of the <scp>T</scp> ibetan <scp>H</scp> imalaya from primary and secondary magnetizations of <scp>J</scp> urassic to <scp>L</scp> ower <scp>C</scp> retaceous sedimentary rocks. Geochemistry, Geophysics, Geosystems, 2015, 16, 77-100.	1.0	51
34	The disappearance of a Late Jurassic remnant sea in the southern Qiangtang Block (Shamuluo) Tj ETQq0 0 0 rgB Palaeoclimatology, Palaeoecology, 2018, 506, 30-47.	T /Overloc 1.0	ck 10 Tf 50 14 51
35	Carbonate-platform response to the Toarcian Oceanic Anoxic Event in the southern hemisphere: Implications for climatic change and biotic platform demise. Earth and Planetary Science Letters, 2018, 489, 59-71.	1.8	49
36	Provenance of the Liuqu Conglomerate in southern Tibet: A Paleogene erosional record of the Himalayan–Tibetan orogen. Sedimentary Geology, 2010, 231, 74-84.	1.0	46

#	Article	IF	CITATIONS
37	Rapid drift of the Tethyan Himalaya terrane before two-stage India-Asia collision. National Science Review, 2021, 8, nwaa173.	4.6	46
38	Two types of hyperthermal events in the Mesozoic-Cenozoic: Environmental impacts, biotic effects, and driving mechanisms. Science China Earth Sciences, 2020, 63, 1041-1058.	2.3	45
39	Stratigraphy of deep-water Cretaceous deposits in Gyangze, southern Tibet, China. Cretaceous Research, 2005, 26, 33-41.	0.6	41
40	Paleogene carbonate microfacies and sandstone provenance (Gamba area, South Tibet): Stratigraphic response to initial India–Asia continental collision. Journal of Asian Earth Sciences, 2015, 104, 39-54.	1.0	38
41	Jurassic carbonate microfacies and relative sea-level changes in the Tethys Himalaya (southern Tibet). Palaeogeography, Palaeoclimatology, Palaeoecology, 2016, 456, 1-20.	1.0	37
42	Remagnetization of carbonate rocks in southern Tibet: Perspectives from rock magnetic and petrographic investigations. Journal of Geophysical Research: Solid Earth, 2017, 122, 2434-2456.	1.4	37
43	Geoscience knowledge graph in the big data era. Science China Earth Sciences, 2021, 64, 1105-1114.	2.3	37
44	Provenance and drainage system of the Early Cretaceous volcanic detritus in the Himalaya as constrained by detrital zircon geochronology. Journal of Palaeogeography, 2015, 4, 85-98.	0.9	36
45	Geology of the Fuding inlier in southeastern China: Implication for late Paleozoic Cathaysian paleogeography. Gondwana Research, 2012, 22, 507-518.	3.0	34
46	Discovery of Middle Jurassic trench deposits in the Bangong-Nujiang suture zone: Implications for the timing of Lhasa-Qiangtang initial collision. Tectonophysics, 2019, 750, 344-358.	0.9	34
47	Himalayan detrital chromian spinels and timing of Indus-Yarlung ophiolite erosion. Tectonophysics, 2014, 621, 60-68.	0.9	33
48	Foraminiferal Biostratigraphy and Palaeoenvironmental Analysis of the Mid-cretaceous Limestones in the Southern Tibetan Plateau. Journal of Foraminiferal Research, 2017, 47, 188-207.	0.1	33
49	Early Cretaceous palaeogeographic evolution of the Coqen Basin in the Lhasa Terrane, southern Tibetan Plateau. Palaeogeography, Palaeoclimatology, Palaeoecology, 2017, 485, 101-118.	1.0	31
50	Shallow-water carbonate responses to the Paleocene–Eocene thermal maximum in the Tethyan Himalaya (southern Tibet): Tectonic and climatic implications. Palaeogeography, Palaeoclimatology, Palaeoecology, 2017, 466, 153-165.	1.0	31
51	New biostratigraphic data from the Cretaceous Bolinxiala Formation in Zanda, southwestern Tibet of China, and their paleogeographic and paleoceanographic implications. Cretaceous Research, 2009, 30, 1005-1018.	0.6	30
52	Upper Cretaceous oceanic red beds in southern Tibet: Lithofacies, environments and colour origin. Science in China Series D: Earth Sciences, 2006, 49, 785-795.	0.9	29
53	Paleoclimatic approach to the origin of the coloring of Turonian pelagic limestones from the Vispi Quarry section (Cretaceous, central Italy). Cretaceous Research, 2009, 30, 1205-1216.	0.6	28
54	Machine learning application to automatically classify heavy minerals in river sand by using SEM/EDS data. Minerals Engineering, 2019, 143, 105899.	1.8	28

#	Article	IF	CITATIONS
55	How faithfully do the geochronological and geochemical signatures of detrital zircon, titanite, rutile and monazite record magmatic and metamorphic events? A case study from the Himalaya and Tibet. Earth-Science Reviews, 2020, 201, 103082.	4.0	28
56	Early cretaceous topographic growth of the Lhasaplano, Tibetan plateau: Constraints from the Damxung conglomerate. Journal of Geophysical Research: Solid Earth, 2017, 122, 5748-5765.	1.4	27
57	Special Topic: Cretaceous greenhouse palaeoclimate and sea-level changes. Science China Earth Sciences, 2017, 60, 1-4.	2.3	27
58	Climatic and tectonic controls on Cretaceous-Palaeogene sea-level changes recorded in the Tarim epicontinental sea. Palaeogeography, Palaeoclimatology, Palaeoecology, 2018, 501, 92-110.	1.0	27
59	Characteristics of Early Eocene radiolarian assemblages of the Saga area, southern Tibet and their constraint on the closure history of the Tethys. Science Bulletin, 2007, 52, 2108-2114.	1.7	26
60	Causes of oxic–anoxic changes in Cretaceous marine environments and their implications for Earth systems—An introduction. Sedimentary Geology, 2011, 235, 1-4.	1.0	22
61	Discovery of the Paleocene-Eocene Thermal Maximum in shallow-marine sediments of the Xigaze forearc basin, Tibet: A record of enhanced extreme precipitation and siliciclastic sediment flux. Palaeogeography, Palaeoclimatology, Palaeoecology, 2021, 562, 110095.	1.0	22
62	Early Eocene sedimentary recycling in the Kailas area, southwestern Tibet: Implications for the initial India–Asia collision. Sedimentary Geology, 2015, 315, 1-13.	1.0	21
63	Paleoceanographic evolution and chronostratigraphy of the Aptian Oceanic Anoxic Event 1a (OAE1a) to oceanic red bed 1 (ORB1) in the Gorgo a Cerbara section (central Italy). Cretaceous Research, 2016, 66, 115-128.	0.6	19
64	Mesozoic Subduction Accretion History in Central Tibet Constrained From Provenance Analysis of the Mugagangri Subduction Complex in the Bangongâ€Nujiang Suture Zone. Tectonics, 2020, 39, e2020TC006144.	1.3	19
65	Preâ€Oxfordian (>163ÂMa) Ophiolite Obduction in Central Tibet. Geophysical Research Letters, 2020, 47, e2019GL086650.	1.5	19
66	Discovery of Upper Cretaceous Neo-Tethyan trench deposits in south Tibet (Luogangcuo Formation). Lithosphere, 2018, 10, 446-459.	0.6	18
67	Sea level, biotic and carbon-isotope response to the Paleocene–Eocene thermal maximum in Tibetan Himalayan platform carbonates. Global and Planetary Change, 2020, 194, 103316.	1.6	18
68	From extension to tectonic inversion: Mid-Cretaceous onset of Andean-type orogeny in the Lhasa block and early topographic growth of Tibet. Bulletin of the Geological Society of America, 2020, 132, 2432-2454.	1.6	18
69	Late Paleozoic magmatism in South China: Oceanic subduction or intracontinental orogeny?. Science Bulletin, 2013, 58, 788-795.	1.7	17
70	Quantitative analysis of iron oxide concentrations within Aptian–Albian cyclic oceanic red beds in ODP Hole 1049C, North Atlantic. Sedimentary Geology, 2011, 235, 91-99.	1.0	16
71	Feasibility of monitoring hydraulic fracturing using time-lapse audio-magnetotellurics. Geophysics, 2012, 77, WB119-WB126.	1.4	16
72	Late Cretaceous evolution of the Coqen Basin (Lhasa terrane) and implications for early topographic growth on the Tibetan Plateau. Bulletin of the Geological Society of America, 0, , B31137.1.	1.6	16

#	Article	IF	CITATIONS
73	Sandstone provenance analysis in Longyan supports the existence of a Late Paleozoic continental arc in South China. Tectonophysics, 2020, 780, 228400.	0.9	16
74	Eustatic and tectonic control on the evolution of the Jurassic North Qiangtang Basin, northern Tibet, China: Impact on the petroleum system. Marine and Petroleum Geology, 2020, 120, 104558.	1.5	15
75	Sandstone memory of a Late Paleozoic continental arc in southeast China (Lower Yangtze region). Chinese Science Bulletin, 2017, 62, 2951-2966.	0.4	15
76	Organic geochemical characterization of Upper Cretaceous oxic oceanic sediments in Tibet, China: a preliminary study. Cretaceous Research, 2005, 26, 65-71.	0.6	14
77	Recognition of trench basins in collisional orogens: Insights from the Yarlung Zangbo suture zone in southern Tibet. Science China Earth Sciences, 2020, 63, 2017-2028.	2.3	14
78	Mineralogical characteristics and geological significance of Albian (Early Cretaceous) glauconite in Zanda, southwestern Tibet, China. Clay Minerals, 2012, 47, 45-58.	0.2	13
79	Discovery of the early Jurassic Gajia mélange in the Bangong–Nujiang suture zone: Southward subduction of the Bangong–Nujiang Ocean?. International Journal of Earth Sciences, 2017, 106, 1277-1288.	0.9	13
80	The major Late Albian transgressive event recorded in the epeiric platform of the Langshan Formation in central Tibet. Geological Society Special Publication, 2020, 498, 211-232.	0.8	12
81	Late Cretaceous to Late Eocene Exhumation in the Nima Area, Central Tibet: Implications for Development of Low Relief Topography of the Tibetan Plateau. Tectonics, 2022, 41, .	1.3	12
82	A multi-task multi-class learning method for automatic identification of heavy minerals from river sand. Computers and Geosciences, 2020, 135, 104403.	2.0	11
83	Upper Cretaceous trench deposits of the Neo-Tethyan subduction zone: Jiachala Formation from Yarlung Zangbo suture zone in Tibet, China. Science China Earth Sciences, 2018, 61, 1204-1220.	2.3	10
84	Paleocene initial indentation and early growth of the Pamir as recorded in the western Tarim Basin. Tectonophysics, 2019, 772, 228207.	0.9	10
85	Initial growth of the Northern Lhasaplano, Tibetan Plateau in the early Late Cretaceous (ca. 92 Ma). Bulletin of the Geological Society of America, 0, , .	1.6	10
86	Late Cretaceous topographic doming caused by initial upwelling of Deccan magmas: Stratigraphic and sedimentological evidence. Bulletin of the Geological Society of America, 2020, 132, 835-849.	1.6	10
87	Climate-driven hydrological change and carbonate platform demise induced by the Paleocene–Eocene Thermal Maximum (southern Pyrenees). Palaeogeography, Palaeoclimatology, Palaeoecology, 2021, 567, 110250.	1.0	9
88	Tracing erosion patterns in South Tibet: Balancing sediment supply to the Yarlung Tsangpo from the Himalaya versus Lhasa Block. Basin Research, 2022, 34, 411-439.	1.3	9
89	Early Jurassic long-term oceanic sulfur-cycle perturbations in the Tibetan Himalaya. Earth and Planetary Science Letters, 2022, 578, 117261.	1.8	9
90	From the southern Gangdese Yeba arc to the Bangong-Nujiang Ocean: Provenance of the Upper Jurassic-Lower Cretaceous Lagongtang Formation (northern Lhasa, Tibet). Palaeogeography, Palaeoclimatology, Palaeoecology, 2022, 588, 110837.	1.0	9

#	ARTICLE	IF	CITATIONS
91	Early Jurassic carbon-isotope perturbations in a shallow-water succession from the Tethys Himalaya, southern hemisphere. Newsletters on Stratigraphy, 2021, 54, 461-481.	0.5	8
92	Geochemistry of intercalated red and gray pelagic shales from the Mazak Formation of Cenomanian age in Czech Republic. Episodes, 2009, 32, 3-12.	0.8	8
93	The Cenomanian-Turonian anoxic event in southern Tibet: A study of organic geochemistry. Diqiu Huaxue, 2001, 20, 289-295.	0.5	7
94	Testing the validity of Nd isotopes as a provenance tool in southern Tibet for constraining the initial India–Asia collision. Journal of Asian Earth Sciences, 2012, 53, 51-58.	1.0	7
95	Petrology and multimineral fingerprinting of modern sand generated from a dissected magmatic arc (Lhasa River, Tibet). , 2018, , .		7
96	Geochemical evidence from the Kioto Carbonate Platform (Tibet) reveals enhanced terrigenous input and deoxygenation during the early Toarcian. Global and Planetary Change, 2022, 215, 103887.	1.6	7
97	Distribution and origin of high magnetic anomalies at Luobusa Ophiolite in Southern Tibet. Science Bulletin, 2014, 59, 2898-2908.	1.7	6
98	Provenance of the Paleozoic to Mesozoic Siliciclastic Rocks of the Istanbul Zone Constrains the Timing of the Rheic Ocean Closure in the Eastern Mediterranean Region. Tectonics, 2021, 40, e2021TC006824.	1.3	6
99	Spatial heterogeneity in carbonate-platform environments and carbon isotope values across the Paleocene–Eocene thermal maximum (Tethys Himalaya, South Tibet). Global and Planetary Change, 2022, 214, 103853.	1.6	6
100	Boron isotope composition of detrital tourmaline: A new tool in provenance analysis. Lithos, 2021, 400-401, 106360.	0.6	5
101	Constraining the timing of Arabia-Eurasia collision in the Zagros orogen by sandstone provenance (Neyriz, Iran). Bulletin of the Geological Society of America, 2022, 134, 1793-1810.	1.6	5
102	基于机器å¦ä¹çš"矿物智能è⁻†å^«æ−¹æ³•ç"ç©¶èչ›å±•ä,Žå±•望. Diqiu Kexue - Zhongguo Dizhi D Geosciences, 2021, 46, 3091.	axue Xueb 0.1	ao/Earth Scie
103	Continental crust recycling in ancient oceanic subduction zone: Geochemical insights from arc basaltic to andesitic rocks and paleo-trench sediments in southern Tibet. Lithos, 2022, 414-415, 106619.	0.6	5
104	Sedimentary Facies, Provenance and Geochronology of the Heshangzhen Group: Implications for the Tectonic Evolution of the Eastern Jiangnan Orogen, South China. Acta Geologica Sinica, 2020, 94, 1138-1158.	0.8	4
105	Enhanced storm-induced turbiditic events during early Paleogene hyperthermals (Arabian continental) Tj ETQq1	1 0,78431 1.6	4 rgBT /Overl
106	Age of Initiation of the Indiaâ€Asia Collision in the Eastâ€Central Himalaya: A Discussion. Journal of Geology, 2006, 114, 637-640.	0.7	3
107	Sedimentological responses to initial continental collision: triggering of sand injection and onset of mass movement in a syn-collisional trench basin, Saga, southern Tibet. Journal of the Geological Society, 2021, 178, .	0.9	3
108	Reply to Comment by W.â€Y. Chen et al. on "Sedimentary and Tectonic Evolution of the Southern Qiangtang Basin: Implications for the Lhasa–Qiangtang Collision Timingâ€. Journal of Geophysical Research: Solid Earth, 2018, 123, 7343-7346.	1.4	2

#	Article	IF	CITATIONS
109	Climateâ€environmental Deteriorations in a Greenhouse Earth System: Causes and Consequences of Shortâ€Term Cretaceous Seaâ€Level Changes (a Report on IGCP 609). Acta Geologica Sinica, 2019, 93, 144-146.	0.8	2
110	Petrogenesis of early Eocene granites and associated mafic enclaves in the Gangdese batholith, Tibet: Implications for net crustal growth in collision zones. Lithos, 2021, 394-395, 106170.	0.6	2
111	Records of latest Triassic, mid-Cretaceous and Cenozoic uplift/exhumation phases in the Istanbul zone revealed by apatite fission-track and (U-Th)/He thermochronology. International Geology Review, 2022, 64, 297-310.	1.1	2
112	Podiform chromite exploration using audio magnetotelluric at Luobusa Ophiolite in Southern Tibet. , 2015, , .		1